Glacier volume and area change by 2050 in high mountain Asia

CrossMark

Liyun Zhao [a], Ran Ding [a], John C. Moore [a,b,c,*]

[a] College of Global Change and Earth System Science, Beijing Normal University, 19 Xinjiekou Wai St., Beijing 100875, China
[b] Arctic Centre, University of Lapland, P.O. Box 122, 96101 Rovaniemi, Finland
[c] Department of Earth Sciences, Uppsala University, Villavägen 16, Uppsala SE-75236, Sweden

ARTICLE INFO

ABSTRACT

We estimate individual area and volume change by 2050 of all 67,028 glaciers, with a total area of 122,969 km^2, delineated in the Randolph Glacier Inventory 2.0 of high mountain Asia (HMA). We used the 25 km resolution regional climate model RegCM 3.0 temperature and precipitation change projections forced by the IPCC A1B scenario. Glacier simulations were based on a novel surface mass balance–altitude parameterization fitted to observational data, and various volume–area scaling approaches using Shuttle Radar Topography Mission surface topography of each individual glacier. We generate mass balance–altitude relations for all the glaciers by region using nearest available glacier measurements. Equilibrium line altitude (ELA) sensitivities to temperature and precipitation change vary by region based on the relative importance of sublimation and melting processes. We also made simulations with mass balance tuned to match satellite observations of glacier thickness changes in HMA from 2003 to 2009. Net mass loss is half as much using the tuned model than using just glaciological calibration data, suggesting the representativity of benchmark glaciers is a larger source of uncertainty in future HMA contributions to sea level rise than errors in glacier inventories or volume–area scaling. Both models predict that about 35% of the glaciers in Karakoram and the northwestern Himalaya are advancing, which is consistent with the observed slight mass gain of glaciers in these regions in recent years. However, we find that 76% of all the glaciers will retreat, most of which are of the maritime type. We project total glacier area loss in high mountain Asia in 2050 to be 22% (in the tuned model) or 35% (un-tuned) of their extent in 2000, and they will contribute 5 mm (tuned model) to global sea level rise.

1. Introduction

High mountain Asia (HMA) possess tens of thousands of mountain glaciers which provide water for many large and important rivers (e.g. Brahmaputra River, Ganges River, Yellow River, Yangtze River, Indus River, Mekong River). Hence their future evolution will have important impacts on the lives of millions of people. There are many studies in the literature monitoring glacier change over time across HMA. The longest records of glacier length and area change since the middle 19th century from across the whole Himalaya and Karakoram were reviewed by Bolch et al. (2012), who found general retreat but a more complex picture in Karakoram, consistent with remote sensing studies reported by Gardelle et al. (2013) for the Karakoram. Sorg et al. (2012) reviewed recent change on glaciers in Tien Shan, finding extensive retreat over the 20th century. Ding et al. (2006) looked at glaciers in China using remote sensing data and maps since the 1950s and report stable conditions in the central and northwestern regions, but extensive retreat in the

periphery of the Tibetan Plateau. Yao et al. (2012) gave a comprehensive overview of mass balance studies on glaciers in the Chinese part of HMA, and additionally a few glaciers have received particularly detailed remote sensing studies (Ye et al., 2006a, b). These authors suggest that most HMA glaciers have retreated over the past few decades with an accelerating shrinkage trend. However, there are significant regional differences in the on-going response of HMA glaciers to climate change. A recent overview based on remote sensing from 2003 to 2009 (Gardner et al., 2013) finds that glaciers are thinning most rapidly in the Himalaya and Tien Shan mountains, moderately thinning in eastern and southern Tibet, and near balance in the western and central portions (Pamir, Karakoram, and western Kunlun). This regional variability in behavior across HMA is also reflected in results from the GRACE satellite gravity observations (Jacob et al., 2012), with no clear net trend and large interannual variability between 2003 and 2010. This is related to ice being converted to water, and Zhang et al. (2013) note a 61% increase in mass derived from GRACE which they explain by increasing lake mass.

Studies focusing on the future response of glacier systems such as HMA to climate change must rely on approaches based on readily available datasets. Previous work has used a mixture of observational and climate forcing of differing sophistication. Radić et al. (2014) used

* Corresponding author at: College of Global Change and Earth System Science, Beijing Normal University, 19 Xinjiekou Wai St., Beijing 100875, China. Tel.: +86 13521460942, +358 400194850.
E-mail address: john.moore.bnu@gmail.com (J.C. Moore).

statistical downscaling of global climate model output (typically at 200 km resolution) to drive individual mass balance of all individual glaciers globally, including HMA, validating and tuning their model regionally with 137 glaciers (10 in HMA) where mass balance measurements exist. This model is essentially a refinement of Radić and Hock (2011), including most relevantly for HMA, improving the annual precipitation bias from climate models to include the seasonal cycle. For HMA, Radić and Hock (2011) suggested a sea level rise contribution from −1 mm to 9 mm, whereas Radić et al. (2014) suggest about 18 ± 5 mm under A1B by 2100. Marzeion et al. (2012) also used a global climate model driven mass balance parameterization, again validated by glaciological observations, finding similar results as Radić et al. (2014), estimating about 15 ± 10 mm of global sea level rise from HMA under RCP6 (which is similar to the A1B scenario) by 2100. Giesen and Oerlemans (2013) estimated glacier sensitivity to changes in temperature and precipitation using an hourly energy-balance approach to parameterize mass balance validated with an 80 glacier global dataset. Under the A1B scenario they estimated the change of glaciers in HMA as 4.8 mm and 20.9 mm of global sea level for the periods 1980–2011 and 2012–2099 respectively. Problems with lack of validation from automatic weather stations in HMA and difficulties with the summer accumulation type of glacier lead to large uncertainties in this approach for HMA.

Even earlier attempts at modeling glacier evolution are notable, but are limited in their spatial coverage. Shi and Liu (2000) estimated the decrease in glacial area for Chinese glaciers over the 21st century by using simple empirical relations between glacier retreat and temperature rise since the Little Ice Age, and predicted shrinkage by 45%–75% by 2100 under a temperature rise of 2 K–4.5 K. Xie et al. (2006) predicted glacier response to climate warming using a complex regional model of glacier mass balance validated by observed areal retreat rates, and concluded that glacier area in China will be reduced by 14%, 40% and 60% by the end of this century under different climate scenarios with temperature increase rates of 0.01, 0.03 and 0.05 °C a^{-1}, respectively.

While the recent decade or so has provided a rich supply of remote sensing products, field measurements of glacier thickness and mass balance are very limited because of the practical and sometimes political difficulties in accessing the glaciers. This pattern of data availability suggests a statistical approach with considerable extrapolation from observations, but with useful constraints from the extensive (but temporally limited) remote sensing data. Furthermore Gardner et al. (2013) observed that estimates of mass loss based on extrapolation from glaciological measurements on the few glaciers studied in HMA tend to produce much larger rates of mass loss than is inferred from the 2009–2003 glacier elevation changes, motivating altimetry data assimilation with statistical modeling as a way forward in projecting future glacier change.

In this article, we propose and apply a simplified method to estimate area and volume change for glaciers in high mountain Asia by 2050 using climate scenarios from a relatively high resolution regional climate model. We make use all the available data including glacier outlines from Randolph Glacier Inventory (RGI) (Arendt et al., 2012), surface elevation from Shuttle Radar Topography Mission (SRTM), glacier equilibrium line altitude (ELA) contour map from the first Chinese glacier inventory, surface mass balance (SMB)–altitude profiles of "benchmark" glaciers, and temperature and precipitation change trend from the 25 km resolution regional climate model coupled to a global climate model running the commonly used A1B forcing scenario. We also differentiate the ELA sensitivity to changes in temperature and precipitation between maritime, sub-continental and continental locations. We calculate volume change for every individual glacier, and convert it to area change by volume–area scaling. This methodology thus makes improvements on previous estimates by using high resolution climate forcing, by making calculations for all glaciers in the region using varying ELA sensitivities, and by using all available SMB data to parameterize the glacier response.

2. Data

The Randolph Glacier Inventory database contains outlines of almost all glaciers and ice caps outside the two ice sheets. We use the data covering South-Asia East, South-Asia West and Central Asia regions from RGI version 2.0 (Arendt et al., 2012). We define these three regions as our HMA study area, containing 122,969 km^2 of glaciated area and a total of 67,028 glaciers (Fig. 1). We calculated the glacier area after correcting for mistaken doubly reported polygons. The RGI data for China, the northern slopes of the Himalayas and the northeastern part of Karakoram are based on topographic maps from the first Chinese glacier inventory (Shi et al., 2009), most of which were made in the 1970s, with some from the 1960s and 1980s. Data in these regions suffer from areal inaccuracies and location uncertainties, and are of heterogeneous but slightly lower quality than the other glacier data in HMA. Most glacier data in HMA from outside China are from the late 1990s or 2000s. For simplicity, we take 1980 and 2000 as the beginning years of our model for glaciers inside, and outside China, respectively.

The Central Asia region contains outlines of glacier complexes rather than individual glaciers, and we do not explicitly correct for this (unlike, for example, Radić et al., 2014). The division of glacier complexes into individual glaciers has an impact on the volume estimate because of the non-linearity of volume scaling relationship (Grinsted, 2013); grouping a glacier complex into a single glacier increases the estimated volume, and we can, to some extent quantify this, by examining a range of volume-area scaling laws. We used the SRTM version 4.1 (void filled version) digital elevation model (DEM) with a horizontal resolution of 90 m to estimate the elevation range spanned by each glacier (Jarvis et al., 2008).

The Chinese Glacier Inventory (Shi, 2005; Chap. 3) provides an ELA contour map (see also Fig. 1 in Yao et al., 2012) over HMA. The ELA on most glaciers was estimated from aerial photogrammetry of glacier shape with the assumption of a convex accumulation region and a concave ablation area (the Hess method) — this is reported to be difficult on small glaciers and fairly subjective. Leonard and Fountain (2003) tested this method on alpine glaciers and found that it worked quite well for detecting the long term ELA (though it was at a slightly lower altitude than the measured ELA). Assuming the glaciers were in steady state through the 1960s and 70s, we take the year 1980 as our ELA reference datum.

Long period variation in ELA can be reconstructed using temperature and precipitation change trends rather than annual variability (e.g. Wang et al., 2010a, b). Here we use the results from the Regional Climate Model Version 3.0 (RegCM3, Fig. 2); the horizontal grid spacing of RegCM3 is 25 km, and the model domain covers all of China and surrounding East Asia areas (Gao et al., 2012). The model makes simulations from 1948 to 2100, a total of 153 years. The RegCM3 model was one-way nested in the 125 km resolution global climate model, MIROC3.2_hires, which was forced using the IPCC A1B greenhouse gas scenario (Meehl et al., 2007). The first three years are used for model spin-up, so the effective range of simulation years spans 1950 to 2100. We make use of results from 1980 to 2050 here. RegCM3 reproduces the present-day (taken to be 1981–2000) observed spatial distribution of surface air temperature and precipitation well (Gao et al., 2012).

3. Methods

We start from known glacier outlines and ELA of all glaciers at the relevant datum years. We take the sensitivity of ELA to temperature and precipitation from energy balance modeling of glaciers in HMA by Rupper and Roe (2008). The mass balance–altitude profile relative to the ELA for each glacier is parameterized from all available measurements on glaciers where SMB is given as a function of altitude. The general approach to evolve the glaciers is a repeated series of annual time steps driven by the regional climate model changes in temperature and precipitation. We use our SMB–altitude profiles to calculate the
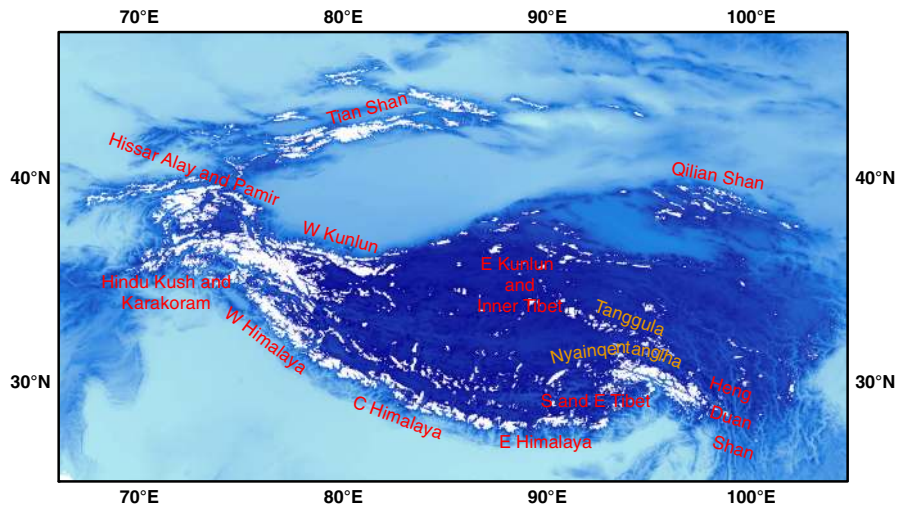
Fig. 1. Spatial distribution of glaciers (in white) and the sub-regions (red text) in South-Asia East, South-Asia West and Central Asia regions from RGI version 2.0. The Tanggula and Nyainqentanglha mountain ranges are also shown (yellow text). (For interpretation of the references to color in this figure legend, the reader is referred to the web version of this article.)

change in mass balance at all elevations on the glacier as climate and ELA change. The whole glacier mass balance gives the volume change rate which can then be converted to an area change rate with volume–area scaling. The area change rate then gives the new glacier altitude distribution for the next round of SMB calculations.

3.1. Volume–area scaling

The method we use to estimate glacier area/volume change is based on volume–area scaling (e.g., Bahr et al., 1997; Radić and Hock, 2010)

$$V = cS^{\gamma}, \tag{1}$$

where V and S are volume (unit: km^3) and surface area (unit: km^2) of a single glacier, c and γ are scaling parameters which vary in different studies in the literature (see Grinsted, 2013 and references therein). The goal of volume–area scaling is to estimate the volume of glaciers in a large sample. Here, we use three sets of parameters, which are

$c = 0.0365$ $km^{3-2\gamma}$, $\gamma = 1.375$ (Radić and Hock, 2010), $c = 0.0380$ $km^{3-2\gamma}$, $\gamma = 1.290$ derived from a least squares log volume regression and $c = 0.0370$ $km^{3-2\gamma}$, $\gamma = 1.314$ from a weighted fit designed to minimize errors in total ice volume (Moore et al., 2013) to study the uncertainties in scaling parameters. Moore et al. (2013) and Grinsted (2013) showed that the volume–area scaling law by Radić and Hock (2010), which derives its exponent, γ from a simplified theoretical analysis (Bahr et al., 1997), has a large bias of the order of 50% relative to observations. The two sets of parameters from Moore et al. (2013) come from volume and area data on 230 separate glaciers. The parameters designed to minimize errors in total volume are most relevant where total ice loss is important, for example in river run-off and sea level rise where mass loss from the small number of large glaciers is much more important than wastage from more numerous smaller ones.

We assume that the mass balance of glacier only comes from SMB, neglecting basal melting and internal process. Required input data include glacier outlines and DEMs which are readily available from RGI
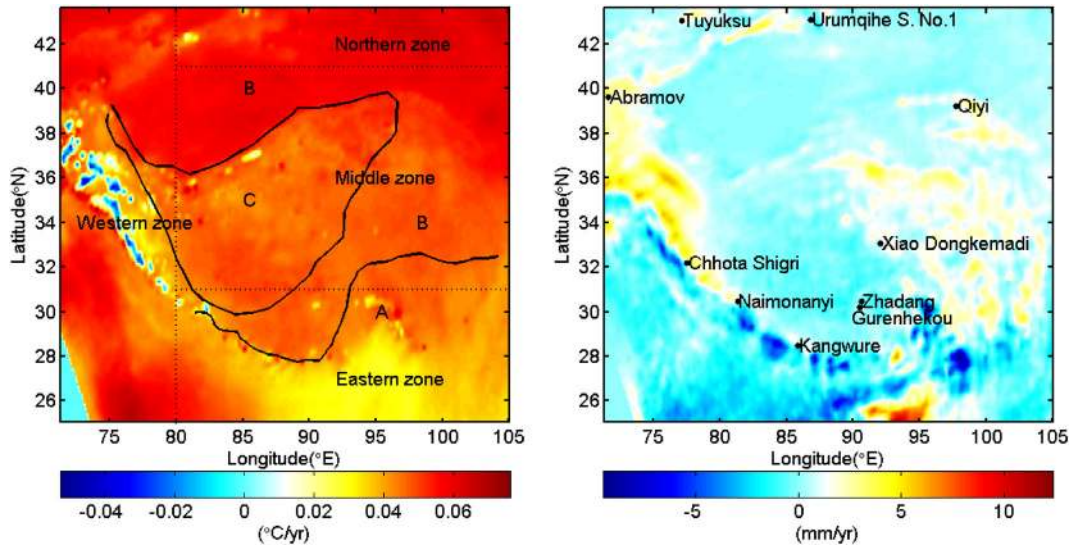

Fig. 2. Averaged change rates of (a) summertime air temperature and (b) annual precipitation from 1980 to 2050 from RegCM3. The solid curves in panel (a) are the boundaries between maritime (A), sub-continental (B) and continental (C) types of glaciers (Shi and Liu, 2000). The dotted lines in panel (a) divide the region into western, eastern, and northern zones used by Rupper and Roe (2008) along with a middle zone they did not define (used in Table 3). Glaciers mentioned in the paper are marked in panel (b).

and SRTM datasets, ELA in a reference year (here we use 1980 as a central year for available data), sensitivity coefficients of ELA change to temperature and precipitation change rate, temperature and precipitation change trend from regional climate model and SMB gradients of typical glaciers. The following procedure is applied to every individual glacier:

Firstly, we make the initialization for the geometry in the year 1980 for glaciers in China and 2000 for glaciers outside China according to our estimates of dates of the RGI data. Glacier area and volume are computed by using glacier outline from RGI dataset and Eq. (1). SRTM DEM data inside the glacier outline are interpolated onto a regular grid with a spatial resolution of 10 m covering the glacier surface. Vertical spacing of altitude bands depends on glacier size, taken as 10 m for glaciers with a total elevation difference from top to bottom larger than 100 m, and one tenth of the glacier altitude difference for glaciers with less altitude range.

The super-index n of the variables in this section denotes the n_{th} year starting from the relevant datum year. The minimum and maximum of surface altitude are denoted as z_{min}^n and z_{max}^n, respectively. The area–altitude distribution function is denoted as $A^n(z)$. The fractional area in each altitude band is approximated by the ratio of grid points in a band to the total grid points in glacier.

Secondly, we calculate SMB $b(z, ELA^n)$ for each glacier, which we assume to be a function of altitude and ELA, using the method described in Section 3.2.

Thirdly, we estimate mass balance B^n in the n_{th} year by

$$B^n = \int_{z_{min}^n}^{z_{max}^n} b(z, ELA^n) \cdot A^n(z) \cdot S^n dz, \qquad (2)$$

for a given SMB profile $b(z, ELA^n)$. We are able to calculate mass balance for each year if we can update S^{n+1}, z_{min}^{n+1}, z_{max}^{n+1} and $A^{n+1}(z)$ once given S^n, z_{min}^n, z_{max}^n and $A^n(z)$. The volume–area scaling formula plays a crucial role here. Eq. (1) can be rewritten as

$$S(t) = c^{-1/\gamma} V(t)^{1/\gamma}. \qquad (3)$$

Taking derivative with respect to t on both sides yields

$$\frac{dS(t)}{dt} = c^{-1/\gamma} \gamma^{-1} V(t)^{1/\gamma-1} \frac{dV(t)}{dt}. \qquad (4)$$

The discrete form of the above equation is

$$S^{n+1} - S^n = c^{-1/\gamma} \gamma^{-1} (V^n)^{1/\gamma-1} B^n, \qquad (5)$$

where we used $B^n = V^{n+1} - V^n$ by definition.

The altitudes of all the grid points are adjusted by using $z_i^{n+1} = z_i^n + b(z_i^n, ELA^n)$ where i denotes the index for grid points. For retreating glaciers, Eq. (5) is used to compute area change. We assume that the area is only lost near glacier terminus. Therefore, the surface altitude maximum in the $n + 1$th year, z_{max}^{n+1}, is the maximum of $\{z_i^{n+1}\}$, but the surface altitude minimum in the $n + 1$th year z_{min}^{n+1} is determined by the area loss percentage since the area loss equals the area occupied by grid points in altitude range $[z_{min}^n, z_{min}^{n+1}]$

$$S^{n+1} - S^n = -S^n \cdot \int_{z_{min}^n}^{z_{min}^{n+1}} A^n(z) dz. \qquad (6)$$

Grid points with the altitude lower than z_{min}^{n+1} are removed from the glaciated area. $A^{n+1}(z)$ is calculated using the updated set of DEM grid points in the $n + 1$th year. For advancing glaciers ($B^n > 0$), volume is changed by using $V^{n+1} = V^n + B^n$, but we assume that the area is unchanged since it is difficult to predict area change for advancing glaciers and the area change also has impact on altitude change of glacier. Therefore, the area changes of advancing glaciers are under-estimated.

3.2. SMB–ELA altitude parameterization

Glaciers in HMA have been grouped into three types (see Fig. 2a) based on regional climate characteristics: the maritime (temperate), sub-continental (sub-polar) and continental (polar) types (Shi and Liu, 2000; Shi, 2005). Shi (2005) reported that there are regional differences in summer mean air temperature and annual precipitation at ELA among the three types of glaciers. The maritime glaciers are mainly located at the southeastern part of HMA, including the eastern Himalayas and the central–eastern part of the Nyainqentanglha Range. The sub-continental glaciers are mainly distributed in the mountain ranges of Tian Shan, the mid-western of the Himalayas, Karakoram and the mid-eastern of Tibet Plateau (including mid-eastern Qilian, eastern Kunlun and Tanggula, and the western Nyainqentanglha Range). The continental glaciers are distributed in the western part of HMA,

Table 1
The benchmark glaciers and their location (Fig. 2b), altitude range, SMB gradients, ELA and SMB data sources.

Glacier name	Location	Altitude range (m)	Averaged SMB gradients	ELA (m)	Period of SMB measurements	Reference
Abramov Glacier	(39°38′N, 71°36′E)	3600–4700	0, z > ELA + 200; 0.0088, z < ELA + 200.	4050–4450	1987–1997	Glacier mass balance bulletin No. 1–6.
Tuyuksu Glacier	(43°03′N, 77°05′E)	3400–4200	0, z > ELA + 100; 0.0057, z < ELA + 100.	3600–4200	1987–2011	Glacier mass balance bulletin No. 1–12.
Urumqihe S. No. 1 Glacier (East branch)	(43°06′N, 86°49′E)	3700–4300	0.002, ELA < z < 4300; 0.01, z < ELA.	3950–4175	1987–2011	Glacier mass balance bulletin No. 1–12.
Naimona'nyi Glacier	(30°27′N, 81°20′E)	5600–6150	0.0006, z > ELA; 0.0038, 5700 < z < ELA.	6100	2005–2010	Yao et al. (2012)
Kangwure Glacier	(28°28′N, 85°49′E)	5700–6100	0.0038, 5700 < z < 6100.	5943	2005–2010	Yao et al. (2012)
Chhota Shigri Glacier	(32°12′N, 77°30′E)	4000–5600	0.003, ELA < z < 5600; 0.01, ELA-150 < z < ELA; 0.005, 4000 < z < ELA-150.	4855–5180	Annual average SMB during 2002–10; 2003–04; 2004–05	Azam et al. (2012), Wagnon et al. (2007)
Xiao Dongkemadi Glacier	(33°04′N, 92°05′E)	5380–5926	0.0003, z > ELA + 65; 0.0048, 5300 < z < ELA + 65.	5515–5750	1989–1994	Fujita et al. (2000)
Zhadang Glacier	(30°28′N, 90°38′E)	5515–6090	0.0037, 5515 < z < ELA.	6024	2005–06; 2009 Jun–Jul; 2009 Sep–2010 May; 2010 Aug–Sep	Zhou et al. (2007), Mölg et al. (2012).
Qiyi Glacier	(39°14′N, 97°45′E)	4310–5145	0.0045, ELA-200 < z < 5300; 0.0018, 4300 < z < ELA-200.	5012	2002 Jun–Sep; 2002–03	Pu et al. (2005)

including the central–western Kunlun Mts. and Tibetan Plateau, eastern Pamir, western parts of Tangula and the Qilian Shan.

Among the glaciers in the region, there are only a few with SMB observations reported in the literature (Fig. 2b). Therefore, it is difficult to use a tailored mass balance model (e.g. Mölg et al., 2012) for each glacier. Instead we use relatively simple SMB parameterizations for the glaciers. We obtain SMB profiles from published articles (Table 1) and find that i) no more than three SMB gradients are sufficient to define SMB profile over elevation range, and ii) a sharp change in SMB gradient occurs near the ELA (illustrated in Fig. 3). Mölg et al. (2012), based on examination of Zhangdang, Xiao Dongkemadi, and Xibu Glaciers, also suggested that a dual SMB profile gradient is a robust feature of glaciers in the central TP (the turning point of gradients is close to ELA), and that this determined more by altitude than by SMB features in any particular year. We also find that SMB gradients depend on altitude rather than glacier location for Naimona'nyi Glacier and Kangwure Glacier, Xiao Dongkemadi Glacier and Zhadang Glacier. Therefore, we construct SMB by using two or three SMB gradients which are estimated from glaciers with in-situ SMB measurements in the region.

The glaciers with SMB measurements used to calculate SMB gradients are shown in Table 1 and plotted on Fig. 3. The HMA covers three glacier regions (Central Asia, South Asia East and South Asia West) in RGI v2, and each of these regions also has sub-regions (see Table 2). Not all sub-regions have glaciers with SMB measurements. Where SMB data exists in the sub-region we use them to parameterize the SMB of all glaciers in that sub-region. Otherwise, we use glaciers from nearby sub-regions which are of the same type (maritime, sub-continental or continental). The choice of benchmark glaciers for each sub-region is shown in Table 2.

For the Hissar Alay and Pamir sub-regions, we use the Abramov Glacier as their benchmark glacier. The observed SMB of Abramov Glacier during 1987–1997 (Fig. 3e) has a constant gradient below around ELA

+ 200 m and stops increasing above the elevation of ELA + 200 m. Therefore, the SMB of glaciers in Hissar Alay and Pamir is parameterized as

$$SMB(z) = \begin{cases} 1.76, & z > ELA + 200 \\ 0.0088(z-ELA), & z \leq ELA + 200 \end{cases}$$

Tuyuksu Glacier and Urumqi S. No. 1 Glacier in Tien Shan have the longest SMB observation periods (1987–2011) among the benchmark glaciers, and are used to model SMB of glaciers in western and eastern Tien Shan, respectively. The SMB–altitude profiles of Tuyuksu Glacier over 1987–2011 are very similar (Fig. 3g), and the SMB was kept constant above ELA + 100 m. The SMB of glaciers in west Tien Shan is parameterized as

$$SMB(z) = \begin{cases} 0.57, & z > ELA + 100 \\ 0.0057(z-ELA), & z \leq ELA + 100 \end{cases}$$

There is always a sharp change in SMB gradients of Urumqi S. No. 1 Glacier (Fig. 3f) near the ELA over 1987–2011, although the observed SMB–altitude profiles vary. We use the mean SMB gradient above and below ELA to construct SMB of glaciers in eastern Tien Shan as

$$SMB(z) = \begin{cases} 0.002(z-ELA), & z \geq ELA \\ 0.01(z-ELA), & z < ELA \end{cases}$$

For the maritime type Himalaya, Hengduan Shan, southern and eastern Tibet sub-regions, we use Naimona'nyi Glacier, Kangwure Glacier and Chhota Shigri Glacier located in the Himalayas (Table 1, Fig. 3a,b). Naimona'nyi Glacier and Kangwure Glacier have almost the same altitude range from 5700 m to 6100 m. The SMB gradient of the two glaciers in [5700, 6100] m is 0.0038. There is no data on SMB above 6100 m, and we assume the SMB gradient there to be the very small value of 0.0006.
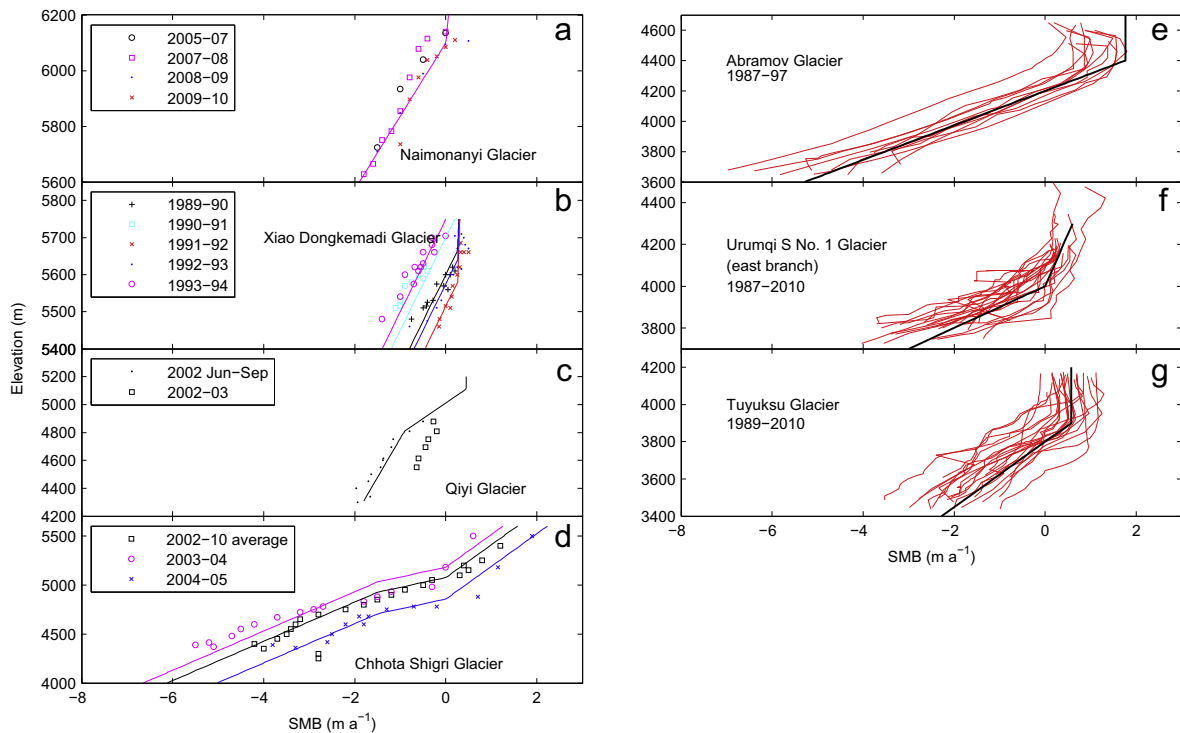

Fig. 3. Observed and modeled SMB of benchmark glaciers in different elevation ranges (see Table 1 and locations in Fig. 2b). a–d: Observed (marker symbols) and modeled (curves) SMB; e–g: Observed (red curves) and modeled (thick black curves) SMB using ELA of 4200 m in panel (e), 4000 m in panel (f) and 3800 m in panel (g). The many mass balance seasons for e–g are listed in Table 1. The observed data are digitized from figures in the references in Table 1. The ELA location is where the SMB = 0, and is generally close to the inflection point in the SMB–altitude relationship. (For interpretation of the references to color in this figure legend, the reader is referred to the web version of this article.)

Table 2
Mean sub-region elevation change between 2003 and 2009 (Gardner et al., 2013) and our simulations with and without tuning SMB gradients below ELA.

Regions in RGI	Sub-region	SMB Glaciers used (Fig. 3)	Elevation change 2003 to 2009 (m a^{-1})			
			Gardner et al. (2013)	Result without tuning	Tuning factor	Result with tuning
Central Asia	Hissar Alay and Pamir	Abramov	-0.13 ± 0.22	-0.59	1/3	0.05
	W Tien Shan	Tuyuksu	-0.58 ± 0.21	-0.69	1	–
	E Tien Shan	Urumqi S. No 1		-0.32	3/2	-0.69
	W Kun Lun	B	0.17 ± 0.15	-0.30	1/4	-0.06
	E Kun Lun and Inner Tibet	B	-0.01 ± 0.12	-0.46	1/4	-0.13
	Qilian Shan	B	-0.32 ± 0.31	-0.72	1/2	-0.36
	S and E Tibet	A	-0.30 ± 0.13	-1.01	1/3	-0.33
South Asia East	Hindu Kush and Karakoram	B	-0.12 ± 0.15	-0.37	1/2	-0.16
	W Himalaya	A	-0.53 ± 0.13	-0.96	1/2	-0.43
South Asia West	C Himalaya	A	-0.44 ± 0.20	-1.74	1/4	-0.41
	E Himalaya	A	-0.89 ± 0.18	-1.41	1/2	-0.80
	Hengduan Shan	A	-0.40 ± 0.41	-1.48	1/4	-0.42

A is a combination of Naimonaiyi and Chhota Shigri Glaciers.
B is a combination of Xiao Dongkemadi and Qiyi Glaciers.

Based on the three glacier profiles, we construct SMB for maritime type of glaciers with ELAs between 5700 m and 6100 m as

$$SMB(z) = \begin{cases} 0.0006(z-6100) + 0.0038(6100-ELA), & z>6100 \\ 0.0038(z-ELA), & 5700<z<6100 \end{cases},$$

and with ELA between 3800 and 5700 m as

$$SMB(z) = \begin{cases} 0.003(z-ELA), & ELA<z<5700 \\ 0.01(z-ELA), & ELA-150<z<ELA \\ 0.005(z-ELA+150), & 3800<z<ELA-150 \end{cases}$$

For the sub-continental and continental sub-regions of western Kun Lun, eastern Kun Lun, Inner Tibet, Qilian Shan, Hindu Kush and Karakoram, SMB data are very limited. Xiao Dongkemadi Glacier (Fig. 3b) is located at the boundary between sub-continental and continental glaciers (Fig. 2), and its SMB gradient in the ablation area is similar to that of Zhadang Glacier. Qiyi Glacier locates in Qilian Shan but has a very poor SMB–altitude observation. Hence we use Xiao Dongkemadi Glacier, Zhadang Glacier and Qiyi Glacier to calculate SMB gradients (Table 2) in both sub-continental and continental regions. There is no SMB data above about 5600 m, and we assume the SMB gradient there to be the very small value of 0.0003. For these sub-regions, we construct SMB function for glaciers with ELAs between 5300 and 5900 m as

$$SMB(z) = \begin{cases} 0.26 + 0.0003(z-ELA-65), & z > ELA+65 \\ 0.004(z-ELA), & 5300< z<ELA+65 \end{cases},$$

with ELA between 4300 and 5300 m as

$$SMB(z) = \begin{cases} 0.45, & z > ELA+100 \\ 0.0045(z-ELA), & ELA-200< z<ELA+100 \\ -0.9 + 0.0018(z-ELA+200), & z<ELA-200 \end{cases}.$$

3.3. ELA–climate relationship

Since ELA is a key glacier feature and varies greatly from glacier to glacier, we must estimate the ELA for each glacier to use the mass balance–ELA–altitude relations detailed in Section 3.2. We interpolate the ELA contour data from the Chinese Glacier Inventory (see Section 2) to get ELA for each glacier in the year 1980. The ELA in the n_{th} year from 1980 is estimated by

$$ELA^n = ELA^{1980} + \alpha \Delta T + \beta \Delta P,$$

where ELA^{1980} is the ELA in 1980, ΔT and ΔP are the net change of summertime air temperature and annual precipitation between 1980 and the n_{th} year, α and β are the sensitivity of ELA shift to air temperature change (unit:°C) and precipitation change (unit: meters), respectively. The averaged change rates of summertime air temperature and annual precipitation from the year 1980 to 2050 are calculated using RegCM3 (Fig. 2). The spatial trend of summertime air temperature shows cooling in the eastern Pamir and northwest Himalaya regions and warming in other areas, while that of annual precipitation increases in the eastern Pamir, Karakoram, eastern TP regions and decreases in the Himalayas over this time interval.

Rupper and Roe (2008) assessed the sensitivity of ELAs to changes in regional climate for Central Asia, and found that ELAs in melt-dominated regions are most sensitive to interannual variability in air temperature, while ELAs in sublimation dominated regions are most sensitive to inter-annual variability in precipitation. In particular, they gave the mean values of ELA sensitivity to summertime air temperature and precipitation for the eastern, western and northern zones of Central Asia (Fig. 1). We apply these values to α and β (Table 3). For the middle zone which Rupper and Roe (2008) do not calculate, we use the averaged value of that in northern and eastern zones. Wang et al. (2010a, b) reconstructed ELA of Qiyi Glacier (Fig. 2) for the period 1958–2008 and analyzed its climate sensitivity, finding that 1 K temperature rise raises ELA by 172 m, which is close to the value of α for sub-continental glaciers.

Table 3
Values of ELA sensitivity to summertime air temperature and precipitation in four zones (Fig. 2).

	Eastern zone	Northern zone	Western zone	Middle zone
Location	[80°E, 105°E] × [25°N, 31°N]	[80°E, 105°E] × [41°N, 50°N]	[60°E, 80°E] × [25°N, 50°N]	[80°E, 105°E] × [31°N, 41°N]
α (m °C^{-1})	321	190	165	255
β (m mm^{-1})	-186	-5540	-680	-2863

Table 4
Estimation of glacier status and glacier volume and area changes from 2000 to 2050 without SMB tuning using volume–area scaling parameters (c, γ in Eq. 1) of 0.0380, 1.290. Sea-level rise assumes ice density of 900 kg m^{-3} and ocean area of 362×10^{12} m^2.

Sub-regions in RGI	Num. of glaciers	Retreating glaciers by 2050 (%)	Total volume in 2050 (km^3)	Volume loss rate (% a^{-1})	Total area in 2050 (km^2)	Area loss rate (% a^{-1})	Global sea level rise 2000–2050 (mm)
Hissar Alay	251	100	17	−1.90	203	−1.85	0.89
Pamir	4521	62	2078	−0.43	10,101	−0.58	1.59
W. Tien Shan	8222	80	885	−0.42	7399	−0.66	0.66
E. Tien Shan	5499	65	234	−0.06	2290	−0.77	0.02
W. Kun Lun	2040	84	2034	−0.09	8511	−0.21	0.28
E. Kun Lun & Inner Tibet	6054	86	1264	−0.39	10,461	−0.45	0.84
Qilian Shan	1311	97	132	−0.71	1212	−0.83	0.20
S. and E. Tibet	2302	98	868	−0.66	3929	−0.81	1.20
Hindu Kush & Karakoram	10,409	68	2056	−0.47	18,750	−0.47	1.75
W. Himalaya	12,413	67	347	−0.79	4862	−0.91	0.62
C. Himalaya	5969	88	212	−1.18	2907	−1.21	0.85
E. Himalaya	4377	88	222	−0.96	2777	−1.04	0.58
Hengduan Shan	3660	93	114	−1.41	1405	−1.47	0.76
All HMA	67,028	76	10,462	−0.52	74,807	−0.70	10.24

4. Results

4.1. Sensitivity to volume–area scaling

We use three sets of volume–area scaling parameters to give a range of estimates for glacier volume and area. The Radić and Hock (2010) parameter set gives consistently the smallest loss rates, while the sea level rise equivalent parameters give slightly greater loss rates than the regression in log space (see Section 3.1 for the values of the parameters). In Table 4 we use the sea level rise equivalent parameters as this gives the smallest sea level rise contribution from HMA, despite having the largest loss rate because this method produces the smallest total ice volumes in HMA. The numbers of retreating, advancing and stationary glaciers are almost the same in all three cases of volume–area scaling. This is because the glacier status (retreating, advancing or stationary) is determined by the sign of mass balance (see Eq. (5) and Fig. 3) rather than the specific volume–area scaling parameters. For the three volume–area scaling methods the contribution to global sea level rise is 10.2–11.4 mm between 2000 and 2050. We predict that glacier total area and volume will decrease at annual averaged rates of 0.65–0.70% and 0.41–0.52% respectively (Table 4). Of the 67,028 glaciers, our results suggest that 24% will be stationary or advancing, and 76% retreating during the period 2000–2050.

4.2. Tuning to glacier elevation change

We can compare the averaged elevation change rate in each sub-region from our simulated glacier evolution with remote sensing estimates (Bolch et al., 2011; Gardelle et al., 2013; Gardner et al., 2013). Gardner et al. (2013) found a heterogeneous pattern of elevation change using satellite imagery between 2003 and 2009, with most rapid thinning (<-0.4 m a^{-1}) in the Himalaya and Tien Shan, moderate rates of thinning (~ -0.3 m a^{-1}) in eastern and southern Tibet, and near balance in the western and central portions of the region (Pamir, Karakoram, and western Kunlun).

We find that our initial simulation result shows a roughly similar pattern to that of Gardner et al. (2013), but our simulation generally gives more negative mass balance and hence elevation changes than the satellite-based estimate. Our modeled average elevation change rate in western Tien Shan is very close to the satellite-based estimate but the largest differences in other sub-regions are by a factor of 4 (Table 2). This is consistent with the finding in Gardner et al. (2013) that satellite-based estimates are significantly less negative than estimates based on spatial interpolation of glaciological and local geodetic measurements, which we in effect use to derive the mass balance parameterizations in Section 3.2.

As our model produces glacier heights each year of the simulation, we can tune our SMB model to try to reproduce the satellite-based elevation change estimates by using a simple multiplier for the SMB gradients below the ELA (Table 2). The resulting volume and area loss rates are less with than without the SMB tuning as expected. The simulated contribution of all the glaciers in HMA to global sea level rise is halved to about 5 mm between 2000 and 2050. Glacier total area and volume are predicted to decrease at annual averaged rates of 0.44% and 0.26%, respectively. The simulation results for all sub-regions with and without tuning SMB are shown in Tables 4 and 5.

Glaciers in Hissar Alay, Himalaya, Hengduan Shan, Tien Shan and Qilian Shan have the most negative modeled volume and area change, which is consistent with the observation that most Himalayan glaciers have been retreating since the mid-19th century (Bolch et al., 2012) and the most negative glacier mass balances now occur along the Himalayas (Yao et al., 2012). Glaciers in southern and eastern Tibet and Hindu Kush and Karakoram have modest modeled volume and area loss. Glaciers in Pamir, Kun Lun and inner Tibet have the smallest modeled volume and area loss.

There are not large differences in relative numbers of glaciers undergoing advance or retreat in the sub-regions with and without SMB tuning. Simulations show that retreating glaciers exist almost everywhere, but are concentrated in Hissar Alay, central and eastern Himalaya, southern and eastern Tibet, Hengduan Shan and Qilian Shan where 90% or more glaciers are predicted to retreat. Advancing glaciers are concentrated in the sub-regions of Hindu Kush and Karakoram, western Himalayas and Pamir where more than 30% of glaciers are predicted to advance (Fig. 4). This is consistent with recently observed stability or mass gain in many Karakoram and northwestern Himalaya glaciers (Hewitt, 2011; Bolch et al., 2012). Sarikaya et al. (2012) also reported that in the eastern Hindu Kush, west of the Karakoram, 25% of the glaciers were stable or advanced between 1976 and 2007.

4.3. Model validation

The annual area shrinkage rate of Akshiirak and Ala Archa glaciers in the northern and central Tien Shan were 0.12% and 0.15% from 1943 to 1977 more than doubling to 0.33% and 0.41% between 1977 and 2003, and annual volume loss rate was 0.24% during 1943–2003 (Aizen et al., 2006). We can simulate the Chinese glaciers from 1980 to compare with these results. We find large differences in rates between eastern and western parts of Tien Shan: in western Tien Shan areal loss rate is 0.45% a^{-1}, which is close to the observation; modeled area loss rate in eastern Tien Shan from 1980 to 2000 is 0.70% a^{-1} without tuning SMB and 0.95% a^{-1} with tuning SMB, both of which are more negative than observed. The simulated volume loss rates of 0.3–0.5% a^{-1} across Tien

Table 5
As Table 4 but with SMB tuning.

Sub-regions in RGI	Num. of glaciers	Retreating glacier by 2050 (%)	Total volume in 2050 (km³)	Volume loss rate (% a⁻¹)	Total area in 2050 (km²)	Area loss rate (% a⁻¹)	Global sea level rise 2000–2050 (mm)
Hissar Alay	251	100	111	−1.34	1005	−1.28	0.63
Pamir	4521	56	2628	−0.06	12,432	−0.29	0.22
W. Tien Shan	8222	80	885	−0.42	7399	−0.66	0.66
E. Tien Shan	5499	73	150	−0.54	2035	−0.85	0.16
W. Kun Lun	2040	77	2106	−0.06	9240	−0.08	0.06
E. Kun Lun & Inner Tibet	6054	83	1520	−0.13	12,991	−0.18	0.28
Qilian Shan	1311	93	167	−0.42	1568	−0.56	0.13
S. and E. Tibet	2302	96	1229	−0.24	5682	−0.39	0.46
Hindu Kush & Karakoram	10,407	65	2349	−0.26	21,210	−0.28	0.97
W. Himalaya	12,413	64	440	−0.47	6003	−0.67	0.38
C. Himalaya	5969	87	397	−0.53	5366	−0.59	0.39
E. Himalaya	4377	86	301	−0.69	3783	−0.78	0.44
Hengduan Shan	3660	75	329	−0.68	4126	−0.75	0.47
All HMA	67,028	74	12,613	−0.26	92,840	−0.44	5.25

Shan are somewhat larger than the observed rate of 0.24%, but the observations from 1943 to 2003 (Aizen et al., 2006) probably mask a much increased rate from 1980.

The modeled annual averaged area and volume loss rates for 2000–2050 of Naimona'nyi Glacier are about 0.3% a⁻¹ and 0.4% a⁻¹, respectively, which is consistent with the observed annual averaged area loss rate of 0.3% a⁻¹ of glaciers in Naimona'nyi region from 1976 to 2003 (Ye et al., 2006a, b). For Kangwure Glacier, the modeled annual averaged area and volume loss rates are about 1.0% a⁻¹ and 1.3% a⁻¹ from 1981 to 2000, respectively, which also match well with the observed rates of 1.0% a⁻¹ and 1.4% a⁻¹ from 1974 to 2008 (Ma et al., 2010). Notably loss rates for both Naimona'nyi Glacier and Kangwure Glacier, are better without tuning than that with SMB tuning. This may well be expected given that SMB data come from these glaciers. The tuning is a way of correcting for the failures of Naimona'nyi Glacier and Kangwure Glacier to represent the regional behavior of glaciers.

We can also compare our results with other remote sensing estimates than the Gardner data we used to tune our SMB. Gardelle et al. (2013) concluded that there was slight mass gain in western Pamir and central Karakoram, and less negative mass balance change in Himalaya than that in Gardner et al. (2013) from a study of nine sites spread from Pamir to eastern Himalaya. Bolch et al. (2011) found average surface lowering rates of 0.36 ± 0.07 m a⁻¹ for ten glaciers in the Nepal Himalaya during 1970–2007 and −0.73 ± 0.45 m a⁻¹ during 2002–2007 using aerial images and satellite data. Pieczonka et al. (2013) obtained overall mass budget of −0.36 ± 0.15 m a⁻¹ for 12 glaciers in central Tien Shan during 1976–2009 and −0.25 ± 0.19 m a⁻¹ during 1999–2009 using satellite imagery, which is about half of the estimate for Tien Shan in Gardner et al. (2013). There are various sources of uncertainties in geodetic mass balance estimate, such as difficulties in identifying glacier ice covered in debris and the poorly constrained penetration of the C-Band SRTM radar signal into snow and ice (Gardelle et al., 2013). The behavior of the glaciers appears to be heterogeneous even over small scales which are probably climatically homogeneous, with factors such as size, topography and debris-cover playing roles. Therefore, remote sensing estimates of mass balance vary according to choice of study site or the sampling of glaciers. Hence, the uncertainties in remote sensing estimates are themselves varied among different regions, and comparable to the differences in Table 2 between the tuned model and the observations of Gardner et al. (2013).

5. Discussion

5.1. Uncertainties

Area and volume change of 67,028 glaciers in HMA for the period 2001–2050 are estimated under the climate scenario A1B predicted by RegCM3 using a combined SMB parameterization and volume–area scaling method, which are based on datasets of glacier outlines, surface topography and ELA. The three sets of volume–area scaling parameters employed yield different glacier volumes and areas but similar annual averaged loss rates. Volume loss rates are reduced by a factor of two when the model is tuned to match recently observed rates of regional glacier down-wasting.

Uncertainties in our results come mainly from 5 aspects:

(1) Data quality of the RGI in China. Large parts of Central Asia, northern slopes of the Himalayas and the northeastern part of Karakoram are covered by the data from the first Chinese glacier inventory, which suffers from the mapping being made over several decades from the 1960s to 1980s, with various inaccuracies due to techniques available at the time. The Central Asia region contains outlines for glacier complexes rather than individual glaciers, but the different volume–area scaling relations we tested change the mass loss rates and sea level rise contributions by only about 10%, suggesting relative insensitivity to mistakes in outlines of particular glaciers. Furthermore the Chinese mapping spanning the 1960s–1980s, which we set to a common datum year of 1980 appears to have produced no glaring regional discrepancies. Our common datum year assumes steady state glaciers, which fortuitously coincides with relative stable climate during the mapping period (Gao et al., 2012).

(2) The scaling parameters in volume–area scaling. The use of different volume–area scaling parameters can produce large difference in glacier volume; however, we find very small uncertainties in glacier shrinkage rate and low sensitivity to sea level rise contributions.

(3) SMB profile. The ELA we estimate for individual glaciers may not be accurate and the SMB gradients we derive from the limited observations may not be representative for all the glaciers in a region. The sensitivity coefficients of ELA to temperature and precipitation change are mean values over the regions. There is a large difference between the simulated glacier response to climate and remote sensing estimates of regional changes in glacier altitude and hence volume loss. This effect has been noted earlier (e.g. Gardner et al., 2013) in the difference between remote sensing studies regional mass balance based on many glaciers compared with glaciological estimates from selected glaciers. We examined this difference by tuning our SMB models to match regional satellite changes. The problem with tuning to remote sensing data is the short time interval of these data, which as well as introducing measurement uncertainties, also cannot address lagged responses from climate forcing to glacier response.
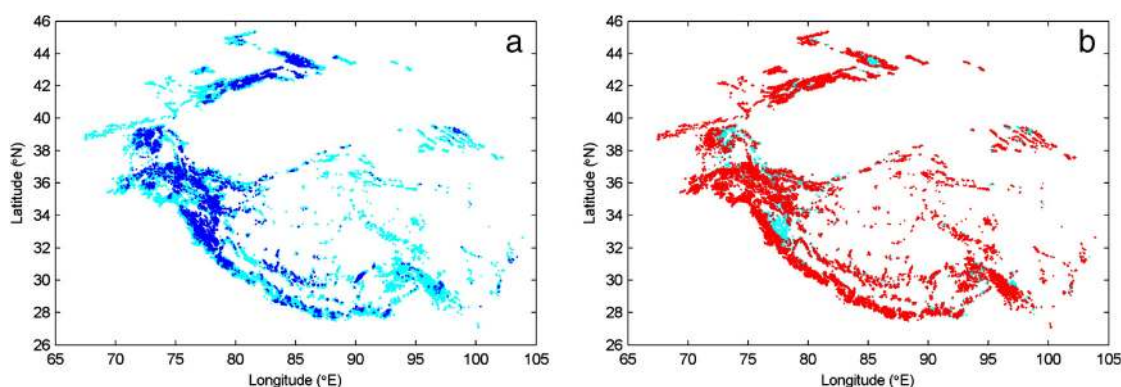
Fig. 4. Spatial distribution of modeled advancing (a; blue) and retreating (b; red) glaciers against the background of all the glaciers (cyan). Note that individual glaciers are too small to be seen in the figures. (For interpretation of the references to color in this figure legend, the reader is referred to the web version of this article.)

(4) The role of ice dynamics in glacier change. Due to the lack of ice thickness data, we cannot use ice flow model to take ice dynamics into account for glacier change. Huss and Farinotti (2012) proposed an approach for calculating thickness distribution based on inversion of surface topography using the principle of flow dynamics. On the other hand, even if we have ice thickness distribution for all the glaciers, it is not computationally practical to simulate ice flow on tens of thousands of glaciers unless the dynamics are extremely simplified which also creates uncertainties. It is helpful to use ice flow modeling on selected glaciers which may then be representative of regional behavior. Zhao et al. (2014) applied a three dimensional, thermo-mechanically coupled full-Stokes model to Gurenhekou Glacier (Nyainqentanglha Range) on Tibetan Plateau to predict glacier change in the next five decades. They also compared the volume changes between with and without dynamics, and found that the SMB plays the dominant role in volume changes compared with ice dynamics. This might not be true for large glaciers, but most glaciers in TP and its surrounding are small like Gurenhekou Glacier.

(5) Uncertainty in climate forcing. The regional climate forcing we use here was forced by the A1B scenario, and these Gao et al. (2012)'s simulations are the only ones we are aware of that cover high mountain Asia at high resolution. We may wonder how does changing the global greenhouse gas forcing scenario or climate model affect climate in the region. Gao et al. (2012) compared simulations using RegCM3 driven by the FvGCM/CCM3 global climate model running the A2 scenario. The global temperatures from the two scenarios are quite comparable at 2050 (e.g., Meehl et al., 2007). The regional climates produced by the two RegCM3 simulations were generally similar over the HMA, even in precipitation changes, but were more different over the monsoon-dominated regions of eastern China. Forcing scenarios diverge much more in the second half of the 21st century than prior to 2050, and the differing model climate sensitivities will also produce a degree of scatter to temperature predictions within any specific scenario (Meehl et al., 2007). High resolution predictions are more important in resolving differences in climate across the glaciated regions (see Fig. 2) than the differences in global temperatures between IPCC scenarios by the year 2050. Furthermore, many analyses of the models show that the climate system behaves linearly within a reasonable temperature range (say 2 °C or so; e.g., Allen and Ingram, 2002; O'Gorman and Schneider, 2008), as do the large ice sheets (e.g., Bindschadler et al., 2013). We may therefore, within the constraints of the available data, assume to a first approximation that glacier loss rates are linear with global temperature. Hence if global temperatures vary somewhat from the 1.6 °C rise at 2050 relative to 1980–2000 average expected under the A2 or A1B scenarios (Meehl et al., 2007), we may expect the high

mountain Asia global sea level contribution of 5 or 10 mm to be similarly scaled.

5.2. Comparison with other studies

Previous estimates of ice volume in HMA range, in terms of sea level equivalent, from 23.8 mm (Huss and Farinotti, 2012), 31.8 mm (Radić et al., 2014) to 37.3 mm (Grinsted, 2013). Here we find using the three volume–area scaling methods that total volumes in the year 2000 are 35, 38 mm and 48.7 mm. It is clear that our volume estimates are larger than the other authors — most likely due to errors in applying glacier scaling laws to glacier complexes (Grinsted, 2013). However, the mass loss rates vary much less between the methods, so calculating the HMA contribution to future global sea level rise is not particularly sensitive to volume–area scaling.

Our estimates (Tables 4 and 5) are of mass loss by 2050. Various authors e.g. Radić et al. (2014) provide estimates of mass loss over the 21st century and show that the response is almost linear over time. At 2050 the sea level rise from HMA estimated by Radić et al. (2014) is about 9 ± 2.5 mm under A1B; Marzeion et al. (2012) estimate about 7.5 ± 5 mm under RCP6 (which is similar to the A1B scenario); Giesen and Oerlemans (2013) estimated about 9 mm. These estimates are generally near our glaciological estimate (Table 4, of 10 mm), but generally higher than our remote-sensing tuned estimate of about 5 mm (Table 5). This is not especially surprising given these earlier studies relied on many of the same benchmark glaciers for model calibration.

There are few estimates of regional and sub-regional glacier loss to compare with our estimates. Xie et al. (2006) predicted that glacier area in China will be reduced by 40% to 60% by the end of this century under different climate scenarios with temperature increase rates of 0.03 and 0.05 °C a^{-1}, respectively. Our RegCM3 rates are intermediate to this range (Fig. 2), and our (un-tuned) area loss by 2050 is 30–33%. Hence our results appear reasonably consistent if loss rates are roughly linear over the century, and also similar to the estimate from Shi and Liu (2000). The relatively short period of change we study means that we have not considered if glacier wastage accelerates or is constant over time. The change rates over time will depend on the hypsometry of individual glaciers, as well as the particular climate evolution it experiences. Here we simply compare the area and volume losses from 2000 to 2050 (Table 4).

Our results show much qualitative consistency with observed regional variations in response to climate change than previous studies, perhaps because of the higher resolution climate forcing we employ. Our model shows that 35% of the glaciers in the vicinity of Pamir, Karakoram and northwestern Himalayas will gain mass from now until 2050, which is consistent with present observational trends. This result is insensitive to model tuning to elevation changes since that approach does not change the sign of the net mass balance. The modeled

area loss rates for individual glaciers (Naimona'nyi and Kangwure Glaciers) also agree well with observations. The results demonstrate the effectiveness of our very simple methodology, particularly the SMB parameterization, though it is applied to all glaciers individually.

The physical reasons for the different behaviors of glaciers across HMA are clearly related to the quite different patterns of climate forcing seen in Fig. 2. In addition to the climate forcing of the SMB profile of the glaciers, their hypsometry and many other factors must play a role. However our model relies on finding the statistical links between climate forcing and glacier response, it cannot directly identify which characteristics are most crucial — and indeed the difference between results tuned to remote sensing and those based purely on glaciological observations shows that many more field measurements are needed to satisfactorily resolve these issues.

Regional differences in loss and gains in glacier volume have implications for river runoff in the glaciated catchments, though details of the runoff increases as glaciers melt and subsequent decreases due to glacier wastage require different modeling approaches that are beyond the scope of this article. Much of the Karakorum is very dry, with local populations relying on irrigation from glacier fed streams. However many glaciers in this region are not expected to shrink, and indeed may expand in coming decades. Thus the area may be more able to bear the impact of climate change on water resources somewhat better than the more maritime and denser populated regions where glacier loss rate is predicted to be much faster.

6. Conclusion

In our study we develop a novel model of glacier response to climate change across high mountain Asia. We differ from previous modeling in using high resolution climate forcing data, and in the parameterizing of the glacier mass balance as a function of changes in ELA based on available field observations. The model produces regionally varying mass balance change in qualitative agreement with observations. However quantitative agreement with observations, while acceptable in some regions, was not very good in many others. We attempted to solve this issue by assimilating remote sensing observations using a simple tuning mechanism to match glacier altitude change with observations. Our results confirm that using just the glaciologically calibrated mass balance produces much higher rates of volume loss than regional loss rates from remote sensing. This discrepancy is due to the lack of representativity of the selected benchmark glaciers compared with other glaciers in the region. It appears that this source of error is much more critical in estimating future changes than errors in the volume–area scaling relation, neglecting glacier dynamics or errors in the glacier mapping inventories.

The contribution to global sea level rise we simulate when tuned to remote sensing data is 5 mm by 2050. This result compares with sea level equivalent losses of about twice of this (10 mm by 2050) using only glaciological calibrated models which are similar as those reported by earlier model studies under A1B-like forcing (Radić et al., 2014; Marzeion et al., 2012; Giesen and Oerlemans, 2013) for HMA.

References

Aizen, V.B., Kuzmichenok, V.A., Surazakov, A.B., Aizen, E.M., 2006. Glacier changes in the central and northern Tien Shan during the last 140 years based on surface and remote-sensing data. Ann. Glaciol. 43, 202–213.

Allen, M.R., Ingram, W.J., 2002. Constraints on future changes in climate and the hydrological cycle. Nature 419, 223–232.

Arendt, A., Bolch, T., Cogley, J.G., Gardner, A., Hagen, J.-O., Hock, R., Kaser, G., Pfeffer, W.T., Moholdt, G., Paul, F., Radić, V., Andreassen, L., Bajracharya, S., Beedle, M., Berthier, E., Bhambri, R., Bliss, A., Brown, I., Burgess, E., Burgess, D., Cawkwell, F., Chinn, T., Copland, L., Davies, B., De Angelis, H., Dolgova, E., Filbert, K., Forester, R., Fountain, A., Frey, H., Giffen, B., Glasser, N., Gurney, S., Hagg, W., Hall, D., Haritashya, U.K., Hartmann, G., Helm, C., Herreid, S., Howat, I., Kapustin, G., Khromova, T., Kienholz, C., Koenig, M., Kohler, J., Kriegel, D., Kutuzov, S., Lavrentiev, I., LeBris, R., Lund, J., Manley, W., Mayer, C., Miles, E., Li, X., Menounos, B., Mercer, A., Moelg, N., Mool, P., Nosenko, G., Negrete, A., Nuth, C., Pettersson, R., Racoviteanu, A., Ranzi, R., Rastner, P., Rau, F., Raup, B.H., Rich, J., Rott, H., Schneider, C., Seliverstov, Y., Sharp, M., Sigurðsson, O., Stokes, C., Wheate, R., Winsvold, S., Wolken, G., Wyatt, F., Zheltyhina, N., 2012. Randolph Glacier Inventory [v2.0]: A Dataset of Global Glacier Outlines. Global Land Ice Measurements from Space. Digital Media, Boulder Colorado, USA.

Azam, M.F., Wagnon, P., Ramanathan, A., Vincent, C., Sharma, P., Arnaud, Y., Linda, A., Pottakkal, G.J., Chevallier, P., Singh, V.B., Berthier, E., 2012. From balance to imbalance: a shift in the dynamic behaviour of Chhota Shigri Glacier (Western Himalaya, India). J. Glaciol. 58 (208), 315–324.

Bahr, D.B., Meier, M.F., Peckham, S.D., 1997. The physical basis of glacier volume–area scaling. J. Geophys. Res. 102 (B9). http://dx.doi.org/10.1029/97JB01696 (20, 355–20, 362).

Bindschadler, R.A., et al., 2013. Ice-sheet model sensitivities to environmental forcing and their use in projecting future sea level (the SeaRISE project). J. Glaciol. 59 (214), 195–224.

Bolch, T., Pieczonka, T., Benn, D.I., 2011. Multi-decadal mass loss of glaciers in the Everest area (Nepal, Himalaya) derived from stereo imagery. Cryosphere 5, 349–358.

Bolch, T., Kulkarni, A., Kääb, A., Huggel, C., Paul, F., Cogley, J.G., Frey, H., Kargel, J.S., Fujita, K., Scheel, M., Bajracharya, S., Stoffel, M., 2012. The state and fate of Himalayan Glaciers. Science 336, 310.

Ding, Y., Liu, S., Li, J., Shangguan, D., 2006. The retreat of glaciers in response to recent climate warming in western China. Ann. Glaciol. 43 (1), 97–105.

Fujita, K., Ageta, Y., Pu, J., Yao, T., 2000. Mass balance of Xiao Dongkemadi glacier on the central Tibetan Plateau from 1989 to 1995. Ann. Glaciol. 31, 159–163.

Gao, X., Shi, Y., Zhang, D., Giorgi, F., 2012. Climate change in China in the 21st century as simulated by a high resolution regional climate model. Chin. Sci. Bull. 57, 1188–1195. http://dx.doi.org/10.1007/s11434-011-4935-8.

Gardelle, J., Berthier, E., Arnaud, Y., Kääb, A., 2013. Region-wide glacier mass balances over the Pamir–Karakoram–Himalaya during 1999–2011. Cryosphere 7, 1263–1286.

Gardner, A.S., Moholdt, G., Cogley, J.G., Wouters, B., Arendt, A.A., Wahr, J., Berthier, E., Hock, R., Pfeffer, W.T., Kaser, G., Ligtenberg, S.R.M., Bolch, T., Sharp, M.J., Hagen, J.O., van den Broeke, M.R., Paul, Frank, 2013. A reconciled estimate of glacier contributions to sea level rise: 2003 to 2009. Science 852–857.

Giesen, R.H., Oerlemans, J., 2013. Climate-model induced differences in the 21st century global and regional glacier contributions to sea-level rise. Clim. Dyn. 41, 3283–3300.

Grinsted, A., 2013. An estimate of global glacier volume. Cryosphere 7, 141–151.

Hewitt, K., 2011. Glacier change, concentration, and elevation effects in the Karakoram Himalaya, Upper Indus Basin. Mt. Res. Dev. 31, 188.

Huss, M., Farinotti, D., 2012. Distributed ice thickness and volume of all glaciers around the globe. J. Geophys. Res. 117. http://dx.doi.org/10.1029/2012JF002523 (F04010).

Jacob, T., Wahr, J., Pfeffer, W.T., Swenson, S., 2012. Recent contributions of glaciers and ice caps to sea level rise. Nature http://dx.doi.org/10.1038/nature10847.

Jarvis, A., Reuter, H.I., Nelson, A., Guevara, E., 2008. Hole-filled Seamless SRTM Data V4. International Centre for Tropical Agriculture (CIAT), (available from http://srtm.csi.cgiar.org).

Leonard, K.C., Fountain, A.G., 2003. Map-based methods for estimating glacier equilibrium-line altitudes. J. Glaciol. 49 (166), 329–336.

Ma, L., Tian, L., Pu, J., Wang, P., 2010. Recent area and ice volume change of Kangwure Glacier in the middle of Himalayas. Chin. Sci. Bull. 55 (20), 2088–2096. http://dx.doi.org/10.1007/s11434-010-3211-7.

Marzeion, B., Jarosch, A.H., Hofer, M., 2012. Past and future sea-level change from the surface mass balance of glaciers. Cryosphere 6, 1295–1322.

Meehl, G.A., Stocker, T.F., Collins, W.D., Friedlingstein, P., Gaye, A.T., Gregory, J.M., Kitoh, A., Knutti, R., Murphy, J.M., Noda, A., Raper, S.C.B., Watterson, I.G., Weaver, A.J., Zhao, Z.-C., 2007. Global climate projections. In: Solomon, S., Qin, D., Manning, M., Chen, Z., Marquis, M., Averyt, K.B., Tignor, M., Miller, H.L. (Eds.), Climate Change 2007: The Physical Science Basis. Contribution of Working Group I to the Fourth Assessment Report of the Intergovernmental Panel on Climate Change. Cambridge University Press, Cambridge, United Kingdom and New York, NY, USA.

Mölg, T., Maussion, F., Yang, W., Scherer, D., 2012. The footprint of Asian monsoon dynamics in the mass and energy balance of a Tibetan glacier. Cryosphere 6, 1445–1461.

Moore, J.C., Grinsted, A., Zwinger, T., Jevrejeva, S., 2013. Semiempirical and process-based global sea level projections. Rev. Geophys. 51, 1–39.

O'Gorman, P.A., Schneider, T., 2008. The hydrological cycle over a wide range of climates simulated with an idealized GCM. J. Clim. 21, 3815–3832. http://dx.doi.org/10.1175/2007JCLI2065.1.

Pieczonka, T., Bolch, T., Wei, J., Liu, S., 2013. Heterogeneous mass loss of glaciers in the Aksu-Tarim Catchment (Central Tien Shan) revealed by 1976 KH-9 Hexagon and 2009 SPOT-5 stereo imagery. Remote Sens. Environ. 130, 233–244.

Pu, J., T. Y., Duan, K., Sakai, A., Fujita, K., Matsuda, Y., 2005. Mass balance of the Qiyi Glacier in the Qilian Mountains: a new observation. J. Glaciol. Geocryol. 27, 199–204 (in Chinese with English abstract).

Radić, V., Hock, R., 2010. Regional and global volumes of glaciers derived from statistical upscaling of glacier inventory data. J. Geophys. Res. 115. http://dx.doi.org/10.1029/2009JF001373 (F01010).

Radić, V., Hock, R., 2011. Regionally differentiated contribution of mountain glaciers and ice caps to future sea-level rise. Nat. Geosci. 4, 91–94. http://dx.doi.org/10.1038/NGEO1052.

Radić, V., Bliss, A., Beedlow, A.C., Hock, R., Miles, E., Cogley, J.G., 2014. Regional and global projections of the 21st century glacier mass changes in response to climate scenarios from GCMs. Clim. Dyn. 42, 37–58. http://dx.doi.org/10.1007/s00382-013-1719-7.

Rupper, S., Roe, G., 2008. Glacier changes and regional climate: a mass and energy balance approach. J. Clim. 21, 5384–5401.

Sarikaya, M.A., Bishop, M.P., Shroder, J.F., Olsenholler, J.A., 2012. Space-based observations of Eastern Hindu Kush glaciers between 1976 and 2007, Afghanistan and Pakistan. Remote Sens. Lett. 3, 77–84.

Shi, Y., 2005. Concise Glacier Inventory of China (in Chinese). Shanghai Popular Science Press.

Shi, Y., Liu, S., 2000. Estimation on the response of glaciers in China to the global warming in the 21st century. Chin. Sci. Bull. 45 (7), 668–672.

Shi, Y., Liu, C., Kang, E., 2009. The Glacier Inventory of China. Annals of Glaciology 50 (53), 1–4.

Sorg, A., Bolch, T., Stoffel, M., Solomina, O., Beniston, M., 2012. Climate change impacts on glaciers and runoff in Tien Shan (Central Asia). Nat. Clim. Chang. 2, 725–731. http://dx.doi.org/10.1038/nclimate1592.

Wagnon, P., Linda, A., Arnaud, Y., Kumar, R., Sharma, P., Vincent, C., Pottakkal, G.J., Berthier, E., Ramanathan, A., Hasnain, S.I., Chevallier, P., 2007. Four years of mass balance on Chhota Shigri Glacier, Himachal Pradesh, India, a new benchmark glacier in the Western Himalaya. J. Glaciol. 53 (183), 603–610.

Wang, N., He, J., Pu, J., Jiang, X., Jing, Z., 2010a. Variations in equilibrium line altitude of the Qiyi Glacier, Qilian Mountains, over the past 50 years (in Chinese with English abstract). Chin. Sci. Bull. 55, 3810–3817. http://dx.doi.org/10.1007/s11434-010-4167-3.

Wang, N., He, J., Pu, J., Jiang, X., Jing, Z., 2010b. Research on Equilibrium Line Altitude change for Qiyi Glacier on Qilian Mountain in the past 50 years (in Chinese). Chin. Sci. Bull. 55 (32), 3107–3115.

Xie, Z., Wang, X., Feng, Q., Kang, E., Liu, C., Li, Q., 2006. Modeling the response of glacier systems to climate warming in China. Ann. Glaciol. 43 (1), 313–316.

Yao, T., Thompson, L., Yang, W., Yu, W., Gao, Y., Guo, X., Yang, X., Zhao, H., Duan, K., Xu, B., Pu, J., Lu, A., Qin, D.H., Xiang, Y., Kattel, D.B., Joswiak, D., 2012. Different glacier status with atmospheric circulations in Tibetan Plateau and surroundings. Nat. Clim. Chang. 15. http://dx.doi.org/10.1038/NCLIMATE1580 (supplementary information).

Ye, Q., Kang, S., Chen, F., Wang, J., 2006a. Monitoring glacier variations on Geladandong mountain, central Tibetan Plateau, from 1969 to 2002 using remote-sensing and GIS technologies. J. Glaciol. 52, 179.

Ye, Q., Yao, T., Kang, S., Chen, F., Wang, J., 2006b. Glacier variations in the Naimona'nyi region, western Himalaya, in the last three decades. Ann. Glaciol. 43 (1), 385–389.

Zhang, G., Yao, T., Xie, H., Kang, S., Lei, Y., 2013. Increased mass over the Tibetan Plateau: from lakes or glaciers? Geophys. Res. Lett. 40 (10), 2125–2130.

Zhao, L., Tian, L., Zwinger, T., Ding, R., Zong, J., Ye, Q., Moore, J.C., 2014. Numerical simulations of Gurenhekou Glacier on the Tibetan Plateau. J. Glaciol. 60 (219), 71–82.

Zhou, G., Yao, T., Kang, S., Pu, J., Tian, L., Yang, W., 2007. Mass balance of the Zhadang Glacier in the central Tibetan Plateau (in Chinese with English abstract). J. Glaciol. Geocryol. 29 (3), 360–365.